Hydrodynamic modeling of Lake Ontario: An intercomparison of three models

Anning Huang,[1,2] Yerubandi R. Rao,[2] Youyu Lu,[3] and Jun Zhao[2]

Received 16 March 2010; revised 22 June 2010; accepted 3 August 2010; published 31 December 2010.

[1] The solutions of three lake hydrodynamic models, namely, Princeton Ocean Model (POM), Canadian Version of Diecast Model, and Estuary, Lake, and Coastal Ocean Model, are compared with each other and with observations in Lake Ontario. The models have the same horizontal resolution and are forced with meteorological observations during mid-April to early October of 2006. The three models obtained qualitatively similar results, although they have differences in physical parameters, numerical scheme, and vertical discretization. Comparison with observations shows that the models can reproduce the time evolution of lake surface temperature reasonably well. All the models produced shallower mixed layers than observations at midlake stations, causing significant errors in simulating the temperatures in the thermocline but performed better near the coast. All the models also reproduced the characteristics of the time variability of the surface currents but quantitatively had substantial errors at subsurface levels. The three models all reproduced the observed spatial pattern of the summer mean near-surface temperatures, with upwelling (colder temperatures) along the north shore and downwelling (warmer temperatures) along the southeastern shore. The models simulated a lake-wide cyclonic circulation occupying a large portion of the lake, consistent with the observed climatology, but showed distinct differences in simulating the smaller gyre in the western corner of the lake. Although POM has half-vertical layers compared to *z* level models, its performance is comparable or slightly better than other models in most of the measures. During a strong easterly wind event, the performances of the models are similar in simulating the upwelling and downwelling processes in the lake and agree with the expected dynamic response to the strong wind forcing.

Citation: Huang, A., Y. R. Rao, Y. Lu, and J. Zhao (2010), Hydrodynamic modeling of Lake Ontario: An intercomparison of three models, *J. Geophys. Res.*, *115*, C12076, doi:10.1029/2010JC006269.

1. Introduction

[2] The Laurentian Great Lakes of North America have horizontal scales of hundreds of kilometers and depth scales of hundreds of meters. Although these lakes are dynamically similar to coastal oceans, they are relatively easier to study because of their smaller size and lack of salinity effects and tides [*Beletsky et al.*, 1997]. The thermal structure and circulation in the Great Lakes vary with the large seasonal variations of surface fluxes [*Boyce et al.*, 1989]. During the winter and spring, the lakes are generally isothermal and the wind forcing can penetrate deep into the water column. In summer and fall, stratification forms in most of the lakes. Because of the large horizontal scale, the *Laurentian Great Lakes* have significant impacts on the local weather and climate [*Anyah and Semazzi*, 2004; *Obolkinm and Potemkin*, 2006]. In turn, atmospheric conditions, such as surface winds and heat flux, precipitation and evaporation, also have significant influences on the thermal structure [*King et al.*, 1997] and water level in lakes [*Hanrahan et al.*, 2010]. So it is necessary to know the 3-D characteristics of temperature and currents because they directly affect the chemical, biological, and ecological processes in these lakes.

[3] Because of these reasons, various attempts have been made over the years to develop 3-D hydrodynamic models for the Great Lakes [e.g., *Bennett*, 1977; *Simons*, 1980], and during the last two decades, 3-D coastal ocean models have been adopted to the Great Lakes. The Princeton Ocean Model (POM) has been used in an operational forecasting system of the Great Lakes [*Schwab and Bedford*, 1994]. POM has been applied to simulate the surface temperature distributions in Lake Erie [*Kuan et al.*, 1994] and the seasonal and interannual variability of circulation and thermal structure in Lake Michigan [*Beletsky and Schwab*, 2001; *Beletsky et al.*, 2006]. Recently, *Huang et al*. [2010] assessed the performance of POM in Lake Ontario with observed forcing and atmospheric forecast forcing in reproducing the circulation and temperature in the lake. The Canadian Version of Diecast Model (CANDIE) was applied to study the seasonal thermal structure

[1]School of Atmospheric Sciences, Nanjing University, Nanjing, China.
[2]National Water Research Institute, Water Science and Technology Directorate, Environment Canada, Burlington, Ontario, Canada.
[3]Bedford Institute of Oceanography, Department of Fisheries and Oceans, Dartmouth, Nova Scotia, Canada.

0148-0227/10/2010JC006269

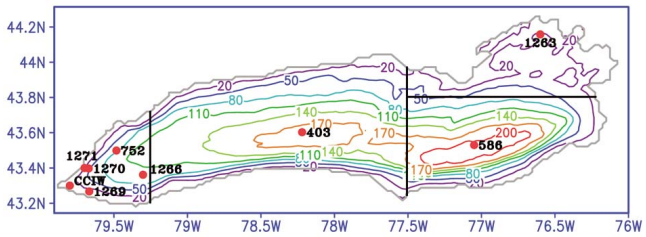

Figure 1. Bathymetry of Lake Ontario (in meters) and the locations of meteorological, water temperature, and ADCP moorings. Horizontal and vertical lines define the regions where the forcing for ELCOM is set to uniform.

and coastal circulation in Lake Huron [*Sheng and Rao*, 2006]. In another study, the Estuary, Lake and Coastal Ocean Model (ELCOM) was used to simulate the thermal structure in the Great Lakes [*Leon et al.*, 2005; *Rao et al.*, 2009]. While these models provided insight into the dynamics of the lakes, little has been done to assess and intercompare their performances with observations in the Great Lakes.

[4] Furthermore, recent studies showed that atmospheric models coupled with 3-D lake models could obtain more realistic local temperature, evaporation, and convergence patterns compared to simulations without lake effects, for example, over Lake Victoria [*Song et al.*, 2004] and Great Bear and Great Slave lakes [*Long et al.*, 2007]. Similar assessment has been carried out with a coupled atmosphere and ocean-ice model in the Gulf of St. Lawrence [*Pellerin et al.*, 2004]. Encouraged by these results, a fully coupled 3-D atmosphere-lake modeling system is being developed by Environment Canada to represent the complex air-lake interaction over the Great Lakes region. Before coupling 3-D lake models with atmospheric models, it is necessary to assess the performance of the lake models with realistic atmospheric forcing in uncoupled mode. In this study, we compare the performance of POM, CANDIE, and ELCOM in Lake Ontario because of their wide application and our previous experience in using these models.

[5] Model intercomparisons have been carried out in various ocean applications. For example, *Beckers et al.* [2002] compared model performances in the simulation of seasonal variations in the Mediterranean Sea; *Chassignet et al.* [2000] compared the performance of five models in the simulation of large-scale characteristics of the North Atlantic circulation. Intercomparisons have also been done on specific numerical aspects [*Baptista et al.*, 1995], turbulent parameterization schemes [*Davies and Xing*, 1995]. Using an idealized setup developed in the Dynamics of Overflows, Mixing, and Entrainment (DOME) initiative, intercomparisons of terrain following (σ layer) and stepped topography (z level) models were conducted [*Mellor et al.*, 2002; *Ezer and Mellor*, 2004]. *Legg et al*. [2006] also used the same DOME setup to compare isopycnal and z level models as well as hydrostatic and nonhydrostatic models. These studies showed the difficulty of resolving near-bottom flows and boundary layer mixing in z level models.

[6] However, in lake applications the intercomparison has been done mainly for 1-D models [*McCormick and Meadows*, 1988]. In one study, POM and a rigid lid version of the Diecast model were intercompared for the simulation of internal Kelvin waves in Lake Michigan [*Beletsky et al.*, 1997]. In contrast to previous studies, we focus on assessing the performances of the 3-D hydrodynamic models in simulating the seasonal and synoptic variability of thermal structure and circulation and make comparison of model results with observations in Lake Ontario. A common model configuration and atmospheric forcing data are setup specifically for this intercomparison study. Furthermore, we assess the capability of models in simulating important physical processes, namely the lake-wide upwelling and downwelling events. The intercomparison would elucidate the relative accuracy of these lake models that would be valuable in judging the suitability of these models for the coupled lake-atmosphere system.

[7] Keeping this in mind, an intensive field investigation was undertaken in Lake Ontario to develop a database of meteorology, temperature, and currents in the lake during the spring to early fall of 2006. The observed meteorological and limnological data in Lake Ontario was discussed by *Huang et al.* [2010]; therefore, only a brief account is provided in section 2. In section 3, we describe the three hydrodynamic lake models and the numerical design for this study in Lake Ontario. The comparisons of model results with observations are presented in sections 4. Section 5 compares the capability of the models in simulating the lake-wide upwelling and downwelling due to the influence of a strong easterly wind event. Section 6 provides a summary of conclusions.

2. Observational Data

[8] The forcing data for the hydrodynamic models includes shortwave radiation, net longwave radiation, surface air temperature, wind speed and direction, and relative humidity, which were observed at four meteorological buoys (CCIW, 403, 586, and 1263, positions shown in Figure 1). Data from the standard weather stations are not used because the records are intermittent and do not include shortwave and longwave radiations. *Huang et al.* [2010] showed that the forcing data developed from these buoys well represented the surface meteorological conditions. Water temperature data were obtained from eight thermistor strings located at stations of 403, 586, 752, 1266, 1269, 1270, 1271, and 1263. At all of these moorings, the Onset Tidbit type thermistors were deployed at 1–3 m intervals in the upper 30 m and 5–10 m apart below this depth. Temperature data were recorded at 60 min intervals with an accuracy of ±0.2°C. Continuous records of vertical profiles of currents were obtained at four stations (1266, 1267, 1269, and 1270) using broadband Acoustic Doppler Current Profilers (ADCP). The velocity profiles were obtained with 1 m bins, except with 5 m bins at station 1266. The accuracy of velocity measurements is on the order of ±0.2%. Daily averages of lake surface temperature, on the basis of measurements with the Advanced Very High Resolution Radiometer (AVHRR), were obtained from NOAA's CoastWatch data set (ftp://coastwatch.glerl.noaa.gov/glsea/avgtemps/2006/glsea-temps2006.dat).

3. Lake Hydrodynamic Models

3.1. POM

[9] The 3-D coastal ocean model POM (latest version, 2008) was originally developed in the 1980s [*Blumberg and Mellor*, 1987]. It solves the conservation equations of heat,

Table 1. Model Specification of Vertical and Horizontal Discretization and Mixing Schemes

	POM	CANDIE	ELCOM
Horizontal diffusion	Smagorinsky parameterization	Smagorinsky parameterization	Constant
Vertical mixing	Level 2.5 Mellor-Yamada scheme	KPP scheme	3-D mixed layer approach
Differencing	Arakawa C grid	Arakawa A grid	Arakawa C grid
Vertical coordinate	σ level (31 levels)	z level (61 levels)	z level (61 levels)
Wind stress	$C_d = (0.8 + 0.065\ \mathrm{WS}) \times 10^{-3}$	$C_d = (0.8 + 0.065\ \mathrm{WS}) \times 10^{-3}$	$C_d = 1.3 \times 10^{-3}$
Shortwave radiation penetration	Jerlov 1	Distribution in top layer	Beer's law with attenuation coefficient 0.2 m^{-1}

mass, and momentum on Arakawa C grid using the finite differencing method. It uses a terrain following vertical coordinate system (i.e., the σ coordinate) scaled on the water column depth. The vertical mixing coefficients are determined by a level 2.5 turbulence closure parameterization [*Mellor and Yamada*, 1982]. In this scheme, the vertical diffusivities for momentum (K_M) and heat (K_H) are defined according to $K_M = lqS_M$ and $K_H = lqS_H$, respectively, where l, the turbulent length scale, and $q^2/2$, the turbulent kinetic energy (TKE), are solved by prognostic equations. The coefficients S_M and S_H are functions of a Richardson number. In addition, the submodel of *Craig and Banner* [1994] whereby breaking wave TKE is injected into the surface [*Mellor and Blumberg*, 2004] is included, but the recent wave-induced mixing [*Mellor*, 2008] is not introduced into this version. POM adopts a mode splitting technique, so that shorter time step is used to solve the barotropic mode associated with the free surface and longer time step is used to solve the baroclinic mode relating to the 3-D temperature, turbulence, and currents. It uses the *Smagorinsky* [1963] eddy parameterization for horizontal diffusion, with the multiplier (horizontal turbulence Prandtl number) set to 0.1 [*Mellor and Blumberg*, 1985]. The optical category of water is set to type I of *Jerlov* [1976] (as shown in Table 1) in the shortwave radiation penetration, which produced better results than other categories [*Huang et al.*, 2010]. Results of *Ezer* [2000] also showed better mixed layer simulations using shortwave radiation penetration compared to net total heat flux. More information of the model is available in the Users' Guide of POM [*Mellor*, 2004].

3.2. CANDIE

[10] CANDIE is a finite differencing, z level model [*Sheng et al.*, 1998; *Lu et al.*, 2001]. It adopts Arakawa A grid using a filtered leapfrog trapezoidal scheme centered in space and time. It adopts the fourth-order numerics suggested by *Dietrich* [1997] and a flux limiter approach suggested by *Thuburn* [1996] in the treatment of the advection terms in the momentum and temperature/salinity equations. CANDIE adopts the parameterization scheme of *Smagorinsky* [1963] for horizontal mixing. The horizontal turbulent Prandtl number is set to 0.1 (same as in POM). For vertical mixing the modified K profile (KPP) scheme of *Large et al.* [1994] is adopted. Following this scheme, the vertical viscosity (K_M) and diffusivity (K_H) are related to the wind stress in the upper mixed layer and to the gradient Richardson number in the stratified interior. The background values are set to $5 \times 10^{-4}\ m^2\ s^{-1}$ for vertical viscosity and $10^{-5}\ m^2\ s^{-1}$ for vertical diffusivity. CANDIE does not adopt the shortwave radiation penetration in exponential decay below the top layer; this component is only distributed in the top layer (as shown in Table 1). The rigid lid version of CANDIE was used by *Sheng and Rao* [2006] to study the circulation and temperature distributions in Lake Huron and Georgian Bay. In this study, a linear free surface version of the model is applied [*Lu et al.*, 2001].

3.3. ELCOM

[11] ELCOM is a free surface, z level model [*Hodges and Dallimore*, 2006]. The fundamental numerical scheme of ELCOM is the TRIM approach [*Casulli and Cheng*, 1992]. The grid stencil is the Arakawa C grid. Wind stress at the surface boundary is modeled as a momentum source distributed evenly over the surface wind mixed layer. Heat exchange through the water's surface is governed by the standard bulk transfer methods. The heat transfer across the surface is separated into nonpenetrative components of longwave radiation, sensible heat transfer, and evaporative heat loss, complemented by penetrative shortwave radiation. Nonpenetrative effects are introduced as sources of temperature in the surface mixed layer, whereas penetrative effects are introduced as source terms in one or more grid layers according to exponential decay and an extinction coefficient (Beer's law; as shown in Table 1). ELCOM adopts 3-D mixed layer approach derived from the mixing energy budgets to simulate the vertical eddy fluxes in momentum and transport equations [*Hodges et al.*, 2000].

3.4. Numerical Design

[12] Table 1 provides a summary of the specification of horizontal/vertical discretization and mixing schemes in the three models. Notably, POM and CANDIE adopt the Smagorinsky scheme for horizontal mixing, but ELCOM uses constant horizontal mixing coefficients. ELCOM was run with typical values of horizontal mixing coefficients in Lake Ontario suggested by *Rao and Murthy* [2001]. However, the model results are not sensitive to the choice of typical values of the horizontal mixing coefficients in lakes. Hence, in this application of ELCOM the horizontal mixing coefficients are set to zero. The vertical mixing schemes used by the three models are all different. Previous ocean model intercomparison studies [e.g., *Ezer and Mellor*, 2004; *Ezer*, 2005] show that z level models have difficulty in resolving the near-bottom flow and boundary layer mixing compared to σ layer models. To minimize this disadvantage, in this study both CANDIE and ELCOM use 61 unevenly spaced vertical levels, with higher resolution (1 m) in the upper 30 m (for better representation of the thermocline and bottom slopes in the coastal area) and coarser resolution (2–10 m) below. POM uses 31 vertical σ levels. A test showed that minor difference in the vertical stratification was caused by changing the number of levels from 31 to 51. This suggests that 31 σ levels are adequate for providing the circulation and thermal structure in the lake. Vertical levels are spaced more closely in the upper 30 m of water to reflect the vertical grid in z level models. The centers of the σ levels are located at −0.0005, −0.0035,

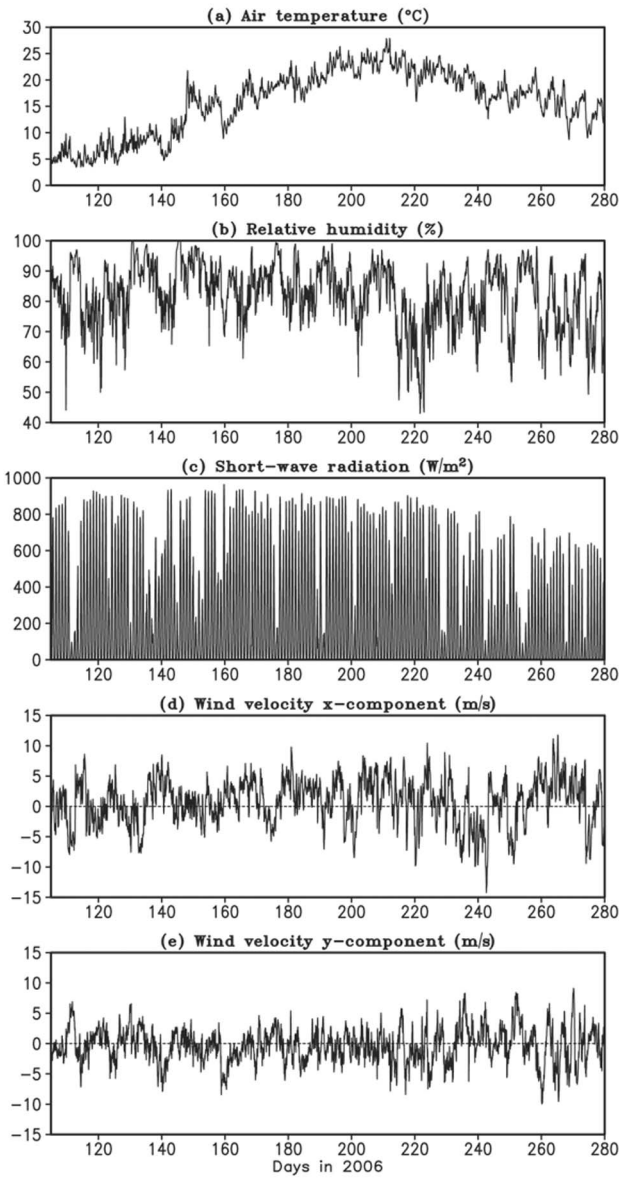

Figure 2. Time series of the hourly mean meteorological parameters at station 403.

−0.013, −0.030, −0.053, −0.073, −0.089, −0.10, −0.12, −0.135, −0.151, −0.165, −0.181, −0.196, −0.212, −0.227, −0.242, −0.269, −0.331, −0.419, −0.506, −0.594, −0.681, −0.78, −0.89, −0.935, −0.955, −0.98, −0.99, and −0.995.

[13] The model domain and bathymetry are shown in Figure 1. All models have a uniform horizontal grid size of 2 km and two open boundaries (i.e., the south and east open boundaries). At the southern open boundary, the mean discharge from Niagara River to Lake Ontario is set to a constant value of 5600 m^3 s^{-1}. At the eastern boundary, the outflows from Lake Ontario into St. Lawrence River are split into the northern exit (2850 m^3/s) and the southern exit (2750 m^3/s). The river temperatures are taken from the nearest grid points in the lake for POM and CANDIE. In ELCOM, the inflow temperatures have to be prescribed. Since measurements of river temperature are not available, we used 3 day averaged air temperature at a station close to the mouth of the Niagara River as the inflow temperature. The observed water temperature at station 1263 was used for the outflow. Because our main objective is not simulating river plumes in the immediate vicinity of the river mouths, these differences in the prescription of river temperature will not have significant impact on the thermal structure or circulation in the lake [*Sheng and Rao*, 2006]. The salinity is set to a constant value of 0.2 parts per thousand in all models. As described by *Huang et al.* [2010], the vertical temperature gradients are very small in early spring; therefore, the initial temperature is simply set as the averaged lake surface temperature observed at four stations (CCIW, 403, 586, and 1263) on 15 April 2006.

[14] The hourly atmospheric forcing data to drive the lake models are derived from the observations at the four meteorological buoys. These include shortwave radiation, net longwave radiation, air temperature, relative humidity, and wind speed and direction. The wind stress is calculated using a variable drag coefficient according to *Large and Pond* [1981] for POM and CANDIE. Following *Laval et al.* [2003], in ELCOM wind stress is calculated using a constant drag coefficient. The surface latent and sensible heat fluxes are calculated using a common bulk formulation [*Fischer et al.*, 1979] during model integration in each model. Surface heat flux components are defined as positive when they tend to heat the lake. Figure 2 shows an example of the time variations of the atmospheric forcing parameters at station 403. All parameters show significant synoptic and seasonal variations; the shortwave radiation also has a significant diurnal variation. Table 2 provides the correlation coefficients between each of the stations CCIW, 586, and 1263 and the station 403 for each atmospheric variable. Among the four stations, the air temperature and shortwave radiation have a high level of consistency. However, the relative humidity, net longwave radiation, and wind components have evident differences. The spatial variability of the atmospheric forcing is considered in setting up the model forcing. For POM and CANDIE, the observed parameters from the four stations are interpolated onto the model grids using a distance weighing method defined as $f = \sum_i (f_i/\alpha_i)/\sum_i (1/\alpha_i)$, where α_i is the distance between the model grids and the ith station and f_i is the value of an observed variable at the ith station. ELCOM was developed for spatially uniform forcing, but limited spatial variability can be incorporated in its latest release. *Laval et al.* [2003] studied the influence of spatial and temporal variations in wind forcing on the circulation in Lake Kinneret with ELCOM. They found that the representation of surface seiches and high-frequency oscillations was improved by introducing the spatial variability. Consequently, in this application of ELCOM, we divide the model domain into four regions (Figure 1), and in each region, the forcing is set to be uniform and equal to the observations at the nearby station.

Table 2. The Correlation Coefficients of Different Atmospheric Variables Between Station 403 and CCIW, 586, and 1263

	CCIW	586	1263
Ta	0.92	0.97	0.94
u	0.73	0.88	0.76
v	0.32	0.79	0.59
SW	0.93	0.94	0.92
RH	0.46	0.84	0.68
NLW	0.68	0.86	0.78

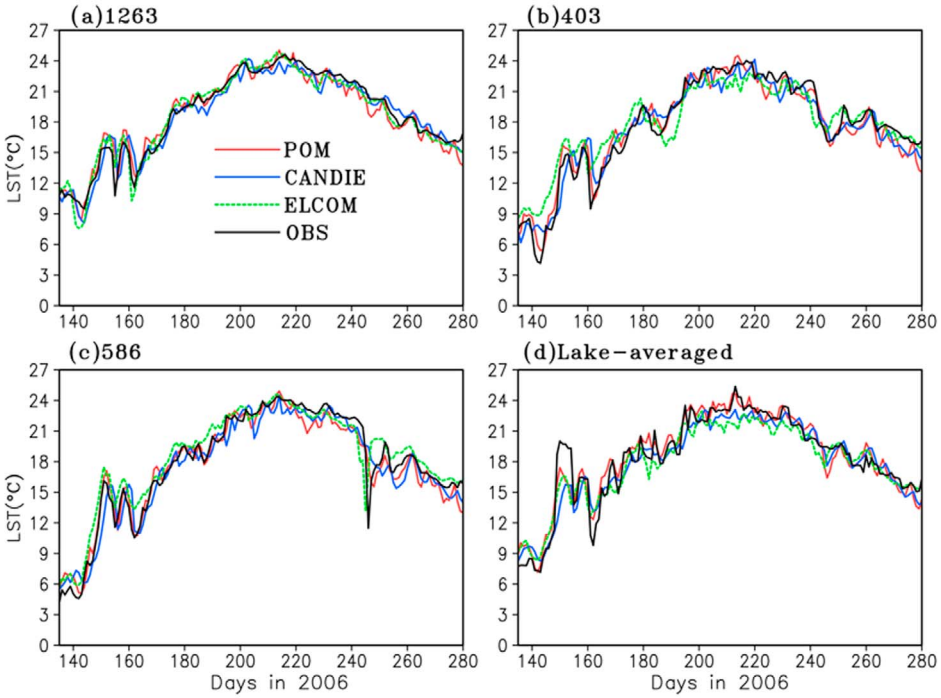

Figure 3. Time series of the observed and simulated lake surface temperature at stations (a) 1263, (b) 403, (c) 586, and (d) the average over the whole lake.

To assess the impact of difference in surface forcing, additional model runs were carried out with uniform surface forcing over the whole lake, and the results of these runs are discussed later.

4. Model Results

[15] All the three lake models are run from 15 April (day 105) to 10 October 2006 (day 283). As discussed by *Beletsky and Schwab* [2001], the typical spin-up time of the lake circulation is relatively short, due mainly to the strong wind-driven character of the lake hydrodynamics. The effect of the initial conditions on the long-term model simulation should be negligible after a few weeks; therefore, the comparisons of observed and simulated variables are made from day 135 to day 283.

4.1. Time Series Comparison of Temperature and Currents

[16] Figure 3 shows the daily averaged time series of lake surface temperature from observations and the three model simulations at stations 403, 586, and 1263 and averaged for the whole lake. The observed lake-averaged surface temperature is derived from the CoastWatch AVHRR data. In general, the simulated seasonal variations of lake surface temperature agree well with observations. Significant variations at synoptic time scales, e.g., a rapid warming and subsequent strong oscillations in spring and rapid cooling and subsequent warming in fall at station 586 are also well simulated. However, differences among models in simulating the surface temperatures at different stations are also evident. For example, ELCOM slightly overestimates the temperatures in spring and underestimates in summer at deeper locations. Both ELCOM and CANDIE underestimate the lake-wide averages in summer, by as large as 2°C–3°C on day 210.

[17] The temporal correlation coefficient (TCC) and root mean square error (RMSE) are used to quantify the agreement between model simulated and observed lake surface temperature. The RMSE is defined as

$$\mathrm{RMSE} = \left(\frac{1}{M} \sum_{i=1}^{M} (f_i^{\mathrm{m}} - f_i^{\mathrm{o}})^2 \right)^{1/2}, \qquad (1)$$

where f_i^{m} and f_i^{o} are modeled and observed water temperature for sample case i (out of M sample cases), respectively. As shown in Table 3, the TCC ranges from 0.94 to 0.98, and the RMSE ranges from 0.85°C to 1.73°C. The three lake models have comparable good performance in simulating the time evolution of lake surface temperature. The performances of POM and CANDIE are close to each other. However, the RMSE values of ELCOM are a little larger than those of POM and CANDIE, except at station 1263. Overall, POM produced

Table 3. Temporal Correlation Coefficients (TCC) and Root Mean Square Errors (RMSE) Between the Modeled and Observed Lake Surface Temperature at Stations 403, 586, and 1263 and the Averages Over the Whole Lake

Sites	TCC			RMSE (°C)		
	POM	CANDIE	ELCOM	POM	CANDIE	ELCOM
403	0.977	0.961	0.959	1.06	1.37	1.73
586	0.979	0.963	0.972	1.12	1.421	1.45
1263	0.981	0.972	0.982	0.89	1.01	0.85
Lake averaged	0.956	0.944	0.951	1.28	1.48	1.51

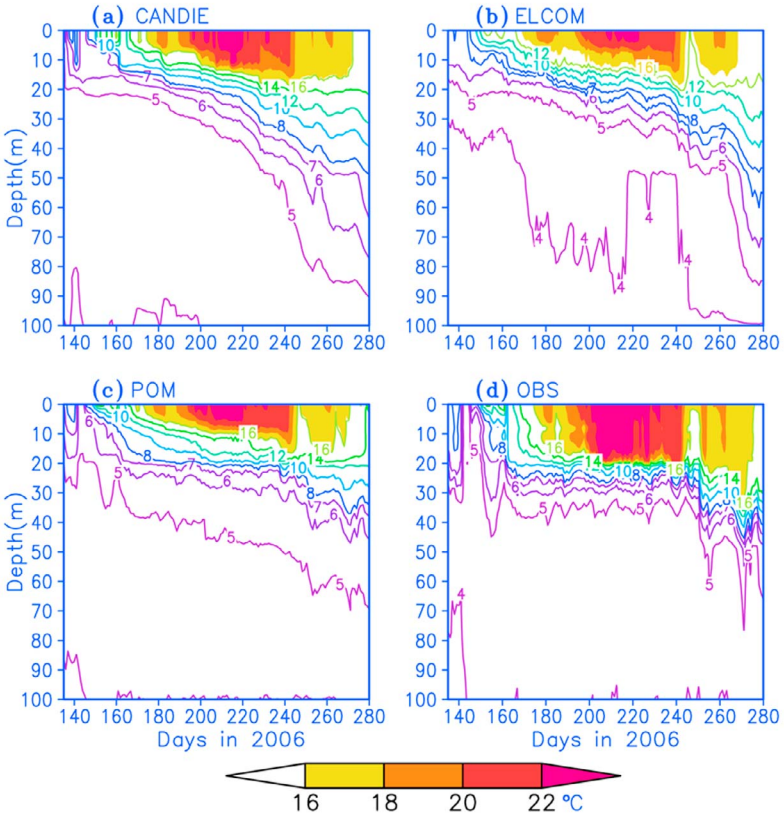

Figure 4. Time-depth distributions of modeled and observed temperatures at site 403.

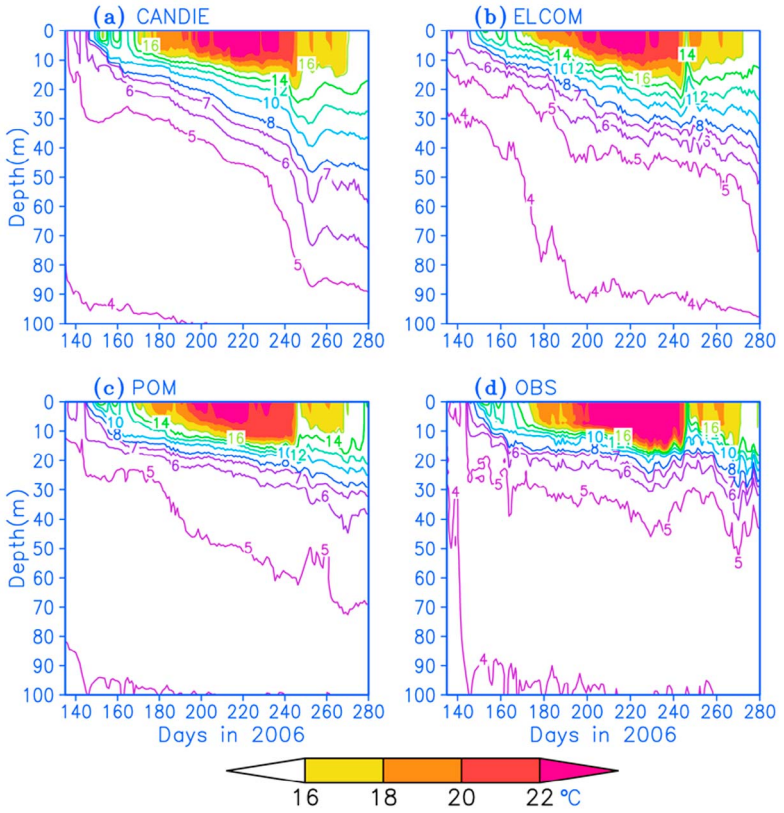

Figure 5. Time-depth distributions of modeled and observed temperatures at site 586.

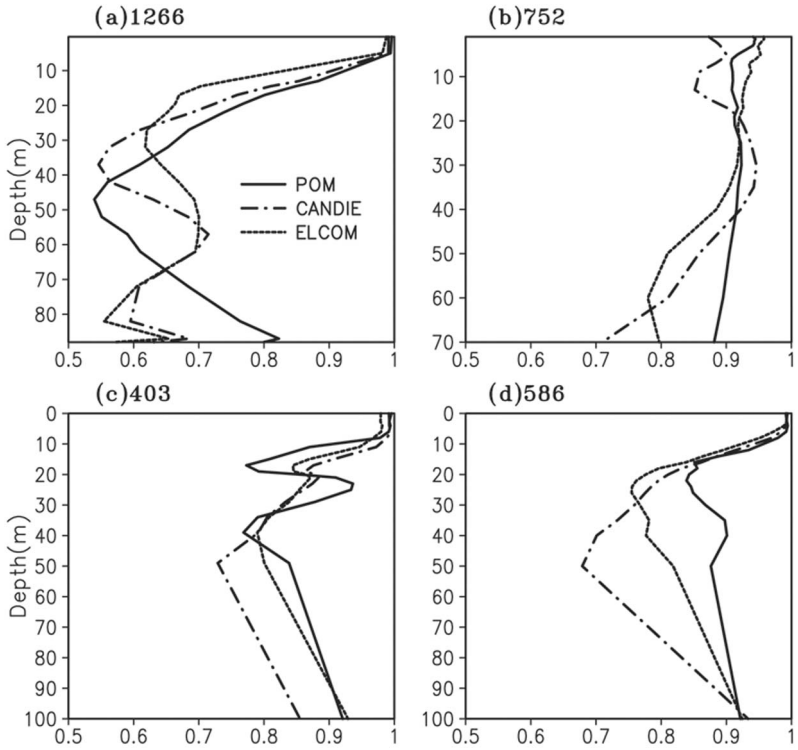

Figure 6. The vertical distributions of temporal correlation coefficients between modeled and observed temperatures at four stations.

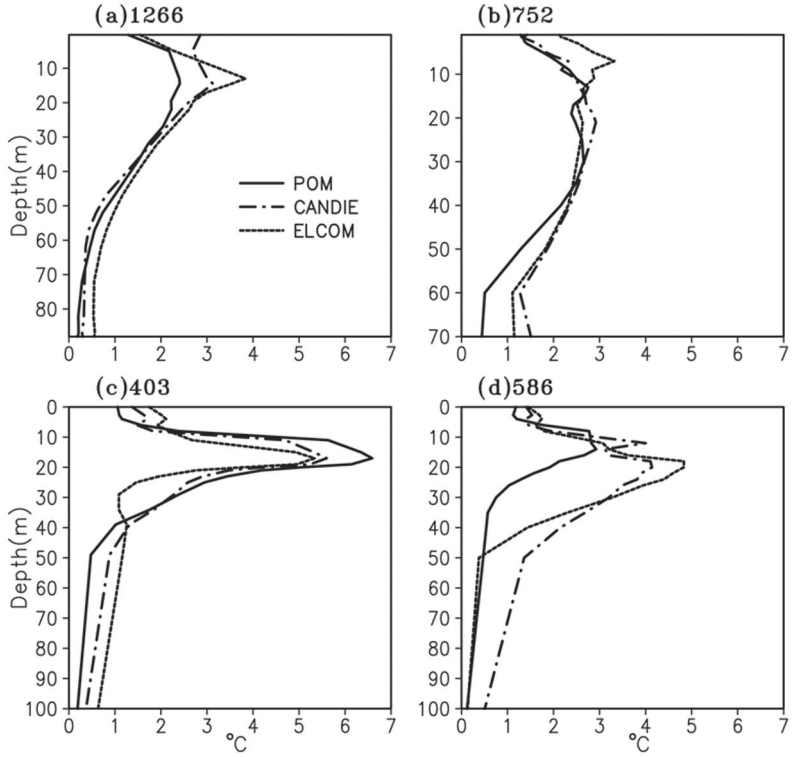

Figure 7. The vertical profiles of root mean square errors between the modeled and observed temperatures at four stations.

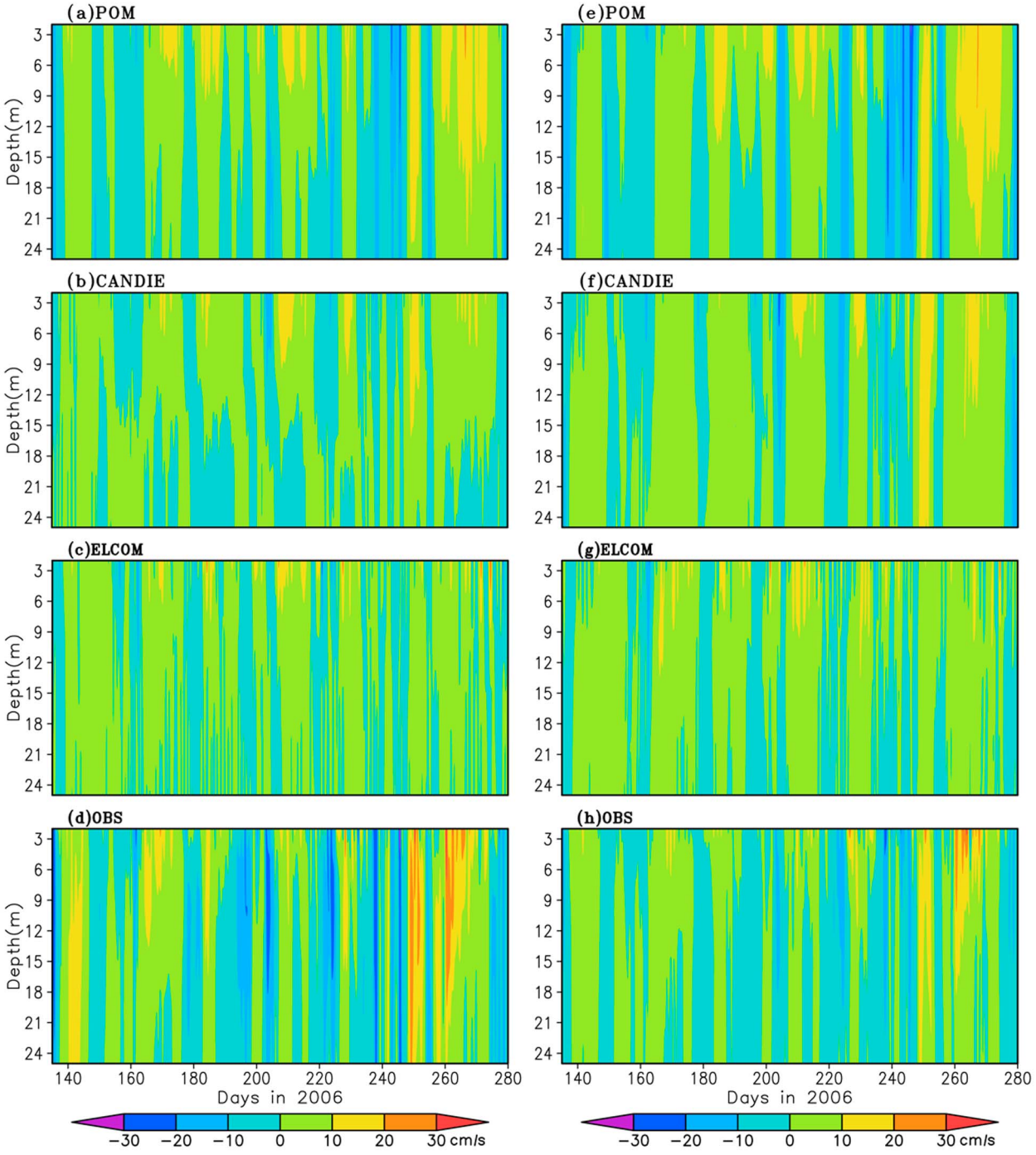

Figure 8. Time-depth distributions of the modeled and observed low-pass filtered (*u*, left) eastward and (v, right) northward components of current velocity at station 1270.

smaller errors in the time variation and magnitude of surface temperatures than the other two models.

[18] The simulation of the vertical structure of temperature is crucial for assessment of climatic effects on lake physics, biology, and water quality. Figures 4 and 5 compare the observed and modeled time-depth variations of temperature structure at sites 403 and 586, located in the deeper area of Lake Ontario (depth > 180 m, figures only show upper 100m). According to observations (Figures 4d and 5d), the lake was isothermal in early spring, stratification started developing in June, and during June to September the lake was stratified with a warm upper mixed layer (temperature difference less than 0.5°C) of 10–20m thick and a cool lower layer. The position of the 13°C isotherm was used to define thermocline depth in Lake Ontario [*Rao and Murthy*, 2001]. A sharp thermocline was established by day 165 at a depth of 20–25 m

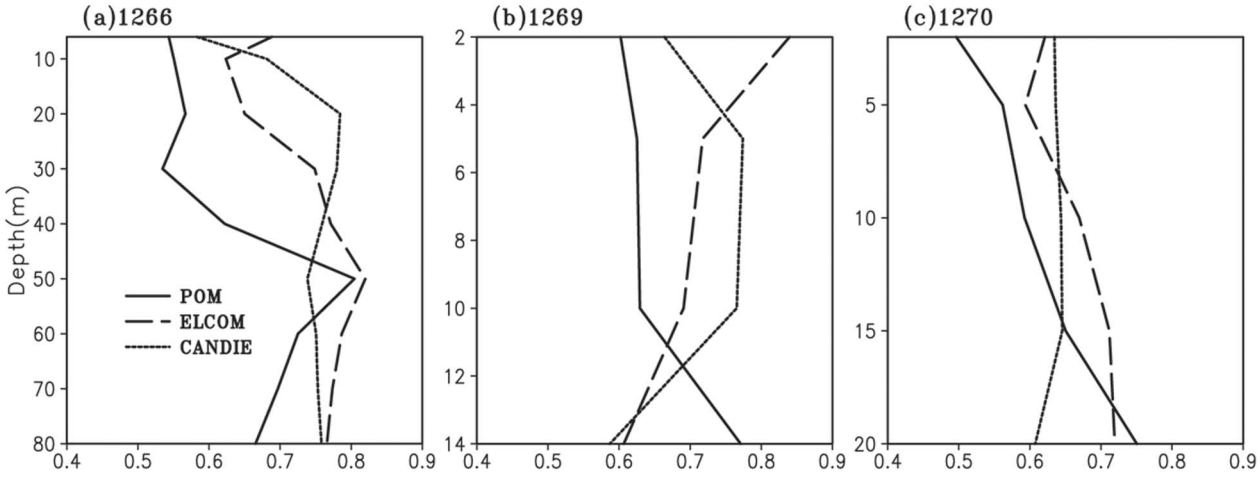

Figure 9. The vertical distribution of normalized Fourier norms between the modeled and observed currents at stations (a) 1266, (b) 1269, and (c) 1270.

at site 403 and a bit shallower (15–20 m) at site 586. Temperatures at depths below 50 m are mostly less than 5°C. Surface heat losses and increased vertical mixing associated with strong winds are responsible for the deepening of the thermocline from late September until the water column is again mixed from top to bottom.

[19] Compared with observations, the simulation by CANDIE (Figures 4a and 5a) shows gradual deepening of the thermocline and slight underestimation of the thickness of the upper mixed layer. However, the modeled thermocline appears to be quite diffusive, as indicated by the 5°C isotherm moving below 50 m by day 230 and the associated warmer than observed temperatures below the thermocline. Figures 4b and 5b show the simulated temperature profiles from ELCOM. ELCOM obtains a mixed layer depth of around 10 m at station 403 and slightly deeper thermocline (15–20 m) at station 586 by day 230. POM obtains similar shallow mixed layers as CANDIE and ELCOM, and the generation and gradual deepening of the thermocline closer to observations (Figures 4c and 5c). Both ELCOM and POM simulate the depth of the 5°C isotherm reasonably well, however, ELCOM obtains slightly colder water temperatures below the depth of 50 m than the observations. The shallower than observed mixed layer from the three models is probably due to insufficient mixing under moderate winds in summer. *Ezer* [2000] noted that shallow thermoclines due to insufficient mixing are common in ocean models, and this is partly caused by neglecting the mixing due to surface wave-induced motions and Langmuir circulation. It is interesting to note that ELCOM and POM generate similar sharp thermoclines at station 403, but at station 586 the thermocline in ELCOM is sharper than that from POM. *Beletsky et al.* [2006] noticed high numerical diffusion in their POM application in Lake Michigan and showed that using higher resolutions did not solve the problem. *Rao et al.* [2009] applied ELCOM for a small embayment in Lake Ontario and obtained reasonable estimates of thermal structure. However, the present application shows that ELCOM also has a tendency of diffused thermocline at some stations.

[20] Figures 6 and 7 show the statistics of temperature comparisons at stations 1266, 752, 403, and 586. These sta-

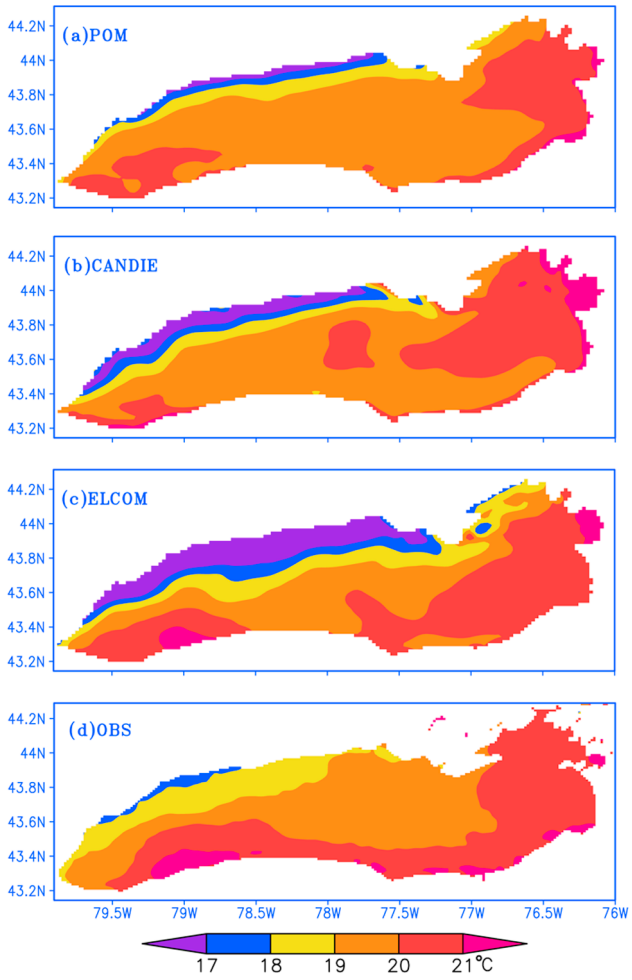

Figure 10. The modeled near-surface (1–3 m) and observed surface temperature distributions during summer (averaged over June-July-August) in Lake Ontario.

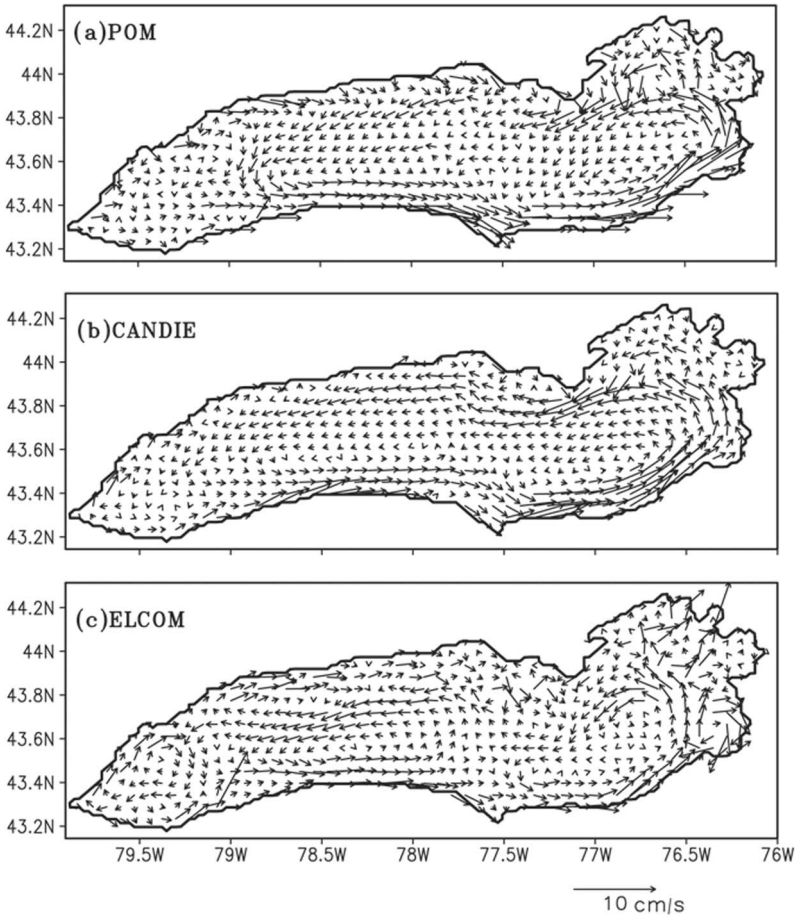

Figure 11. The modeled depth-averaged currents during the summer of 2006.

tions represent conditions from shallow to deep depths. As shown in Figure 6, the correlations between the observed and modeled temperatures are over 0.9 above the depth of 5 m; however, the correlations in the thermocline area are much smaller than those at other depths. POM obtains slightly higher correlations than other models except at station 403. As shown in Figure 7, all the models produce larger RMSE values in the thermocline than at other depths. At station 403, all models obtain large RMSE values, up to 5°C–6°C, in the thermocline. This is related to the too shallow mixed layer in model solutions, as shown in Figure 4.

[21] The model solutions are further evaluated by comparing the simulated and observed currents at all ADCP stations. Figure 8 shows the time-depth distributions of hourly velocities at station 1270. A low-pass filtering with a cutoff at 24 h has been applied to both the modeled and observed currents. The observations show that the flow at this location was directed to the southwest during most of the time between days 140 and 280 in 2006 (Figures 8d and 8h). The current speed increased to a maximum 0.4 m s^{-1} from days 250 to 270. All the three models reproduced the characteristics of the time-depth distributions of the observed currents. However, the models underestimated the current velocity at subsurface depths. Compared to CANDIE and ELCOM, the simulated current speeds from POM agree better with observations, notably between days 250 and 270.

[22] To quantify the model performance in simulating currents, we followed *Beletsky et al.* [2006] to calculate the misfit between the modeled and observed currents represented by

$$Fn = \left(\frac{1}{M}\sum_{t=\Delta t}^{M\Delta t}\left|\overrightarrow{V_{\mathrm{m}}} - \overrightarrow{V_{\mathrm{o}}}\right|^2\right)^{\frac{1}{2}} \Big/ \left(\frac{1}{M}\sum_{t=\Delta t}^{M\Delta t}\left|\overrightarrow{V_o}\right|^2\right)^{\frac{1}{2}}, \qquad (2)$$

where $\overrightarrow{V_{\mathrm{m}}}$ and $\overrightarrow{V_{\mathrm{o}}}$ are modeled and observed currents, respectively. *Fn* is a normalized Fourier norm and can also be regarded as the relative percentage of variance in the observed currents that is unexplained by the model solutions. The smaller the *Fn*, the better the model results fit the observations. As shown in Figure 9, *Fn* ranges from 0.4 to 0.9 at the three ADCP stations for the daily currents modeled by the three lake models. It shows that POM performed slightly better than ELCOM and CANDIE in simulating the currents.

4.2. Spatial Distribution of Thermal Structure and Currents

[23] In large lakes such as the Great Lakes, the surface temperature has significant spatial variability, due to the influence of currents that can transport and redistribute the heat obtained from atmosphere both horizontally and vertically [*Lam and Schertzer*, 1999]. Figure 10 shows the summer mean (June-July-August) near-surface (1–3 m) temperatures

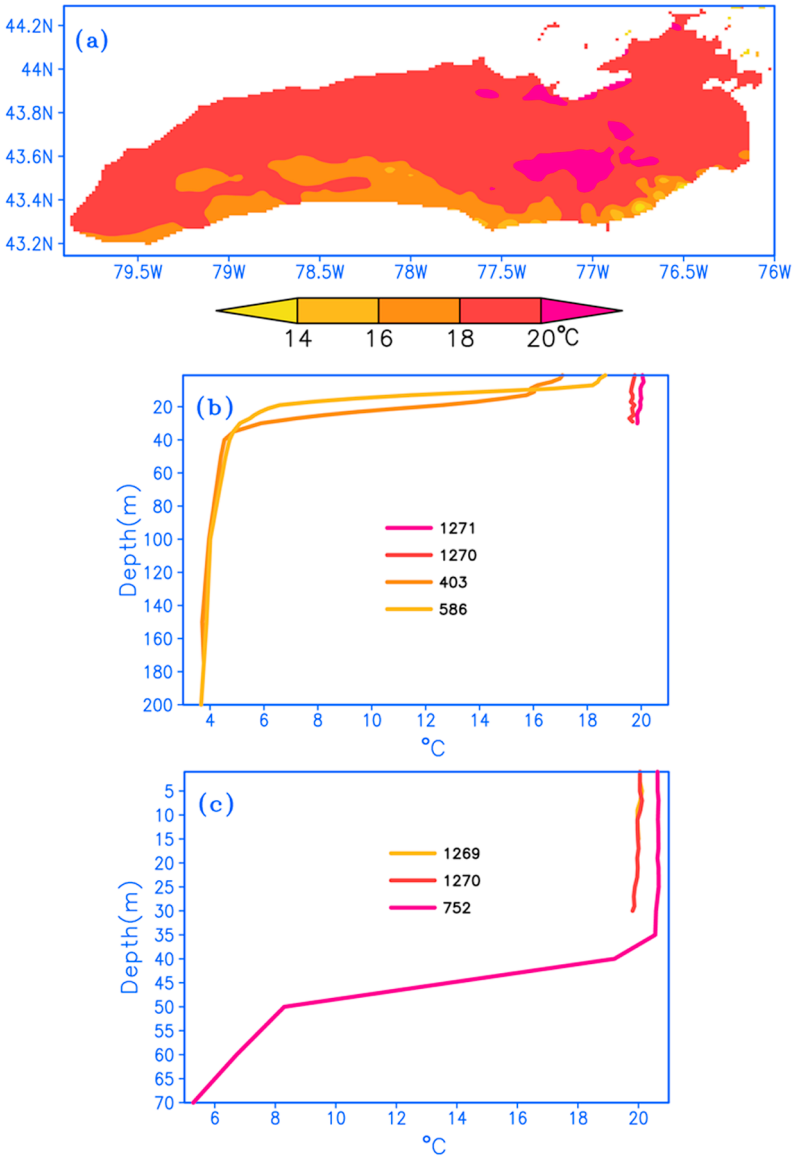

Figure 12. The observed daily averaged (a) surface temperature and (b and c) vertical profiles of temperature in Lake Ontario on 1 September 2006.

from POM, CANDIE, and ELCOM. The AVHRR surface temperatures obtained from CoastWatch are also averaged for this period to provide observational verification to the models (Figure 10d). The observed temperature gradually increases from northwest to southeast: less than 18°C and over 20°C in the northwestern part and southern and eastern parts of the lake, respectively. This spatial distribution is mainly a consequence of the prevailing winds from the west and northwest in summer over the lake, which causes upwelling along the northwestern shore and downwelling along the southeastern shore. The modeled summer mean near-surface temperatures (Figures 10a–10c) show similar spatial distribution as observations. In the northwestern part of the lake, the temperatures from the three models are cooler than the observed values by 1°C–2°C. The models obtain larger areas of upwelling than the observed one. One possible reason of the discrepancy between model solutions and observations is that the satellite observations of skin temperature can be higher than the surface layer temperature as simulated by the model.

[24] *Beletsky et al.* [1999] noted that in Lake Ontario, the summer mean circulation consists of a combination of a large cyclonic gyre with maximum current speed of 2.5 cm s^{-1} and a smaller anticyclonic gyre in the western part of the lake. As shown in Figure 11, all the models simulated a distinct cyclonic circulation occupying a large portion of the lake. ELCOM and POM also obtained a smaller anticyclonic gyre in the western end of the lake. Mean currents obtained are in the order of 2–7cm s^{-1}, which are in good agreement with observed currents in the lake [*Saylor et al.*, 1981; *Beletsky et al.*, 1999]. ELCOM also simulated additional smaller gyres at the eastern end and along the north shore of the lake, which cannot be confirmed by available observations.

[25] One may ask whether the differences among model solutions can be caused by the slight differences in the surface

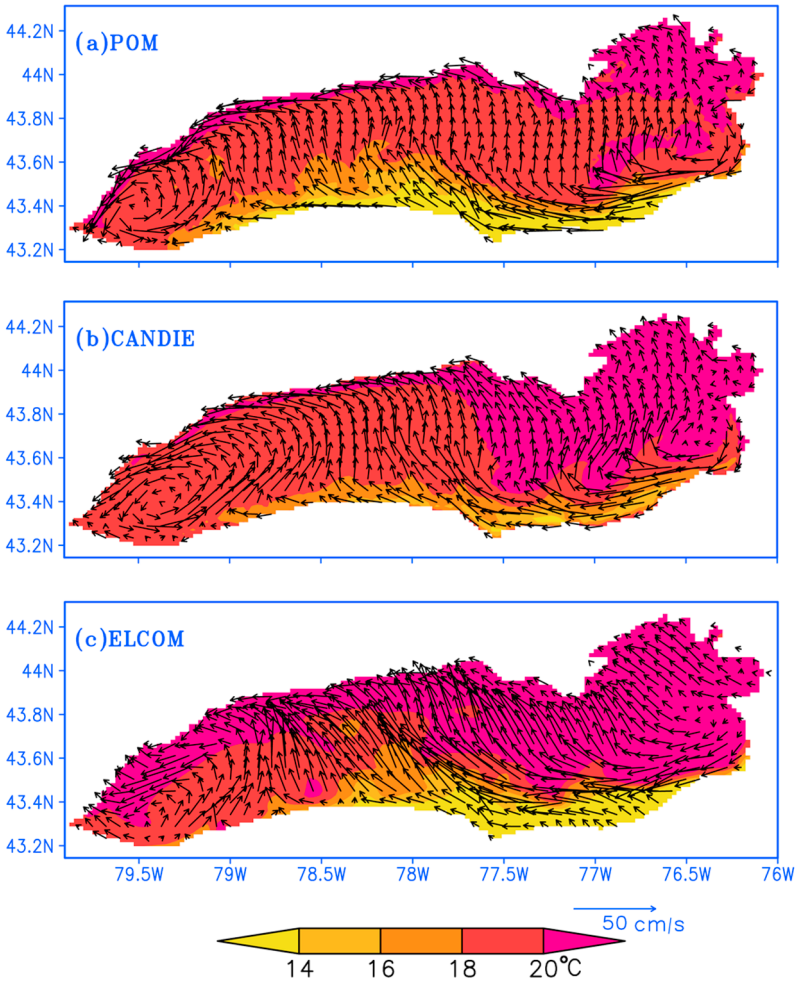

Figure 13. The modeled daily averaged near-surface (1–2 m) temperature (shaded) and currents (vectors) in Lake Ontario on 1 September 2006.

forcing fields mentioned in section 3.4. To answer this question, additional simulations were carried out by running the models with spatially uniform surface forcing. The results showed that the three models obtained similar distribution of temperatures. In terms of the summer mean depth-averaged circulation, POM and CANDIE obtained two counter-rotating gyres, and ELCOM produced multiple gyres similar to the results with spatially variable winds (figures not shown). This suggests that the differences among the model solutions can be mostly accounted for by the differences in model physics/numerics and vertical grid setup.

5. Easterly Wind Event and Associated Downwelling and Upwelling

[26] During summer when the lake is stratified, strong wind events will cause upwelling and downwelling of the thermocline along the shore. The scale of the offshore distance over which these events takes place, typically 5–10 km, is related to the wind stress and nearshore bathymetry. Upwelling and downwelling can produce large onshore-offshore transport of material; hence, it is essential that they are reproduced by 3-D lake models. The three models have a horizontal resolution of 2 km, so it is expected that the dynamics of upwelling and downwelling will be captured. However, *Beletsky et al.* [1997] pointed out that such resolution may not fully resolve the dynamics of internal Kelvin waves.

[27] To evaluate the performance of the models in simulating the upwelling and downwelling processes, we examine the strongest wind event on 1 September 2006 (day 244). During this day, the daily southeasterly wind speed reached over 11 m s^{-1} over the whole lake. Figure 12a shows the observed surface temperatures from CoastWatch data. The temperatures increased from the southern coast to the north. The temperature was about 16°C–18°C along the southern coast, with patches of 14°C–16°C along the southeast part. In other parts of the lake, the temperatures ranged from 18°C to 20°C. This spatial distribution is mainly a consequence of the southeasterly wind, which caused upwelling along the southeastern shoreline and downwelling along the northern shoreline. Figures 12b and 12c show the daily averaged vertical profiles of temperature obtained from mooring observations. The thermocline was located at about 30 m at station 586 in the eastern central basin, and below 40 m at station 752 in the western end of the lake. This indicates downwelling in the regions near station 752.

[28] The model simulated spatial distributions of surface temperatures are shown in Figure 13. All models reproduced

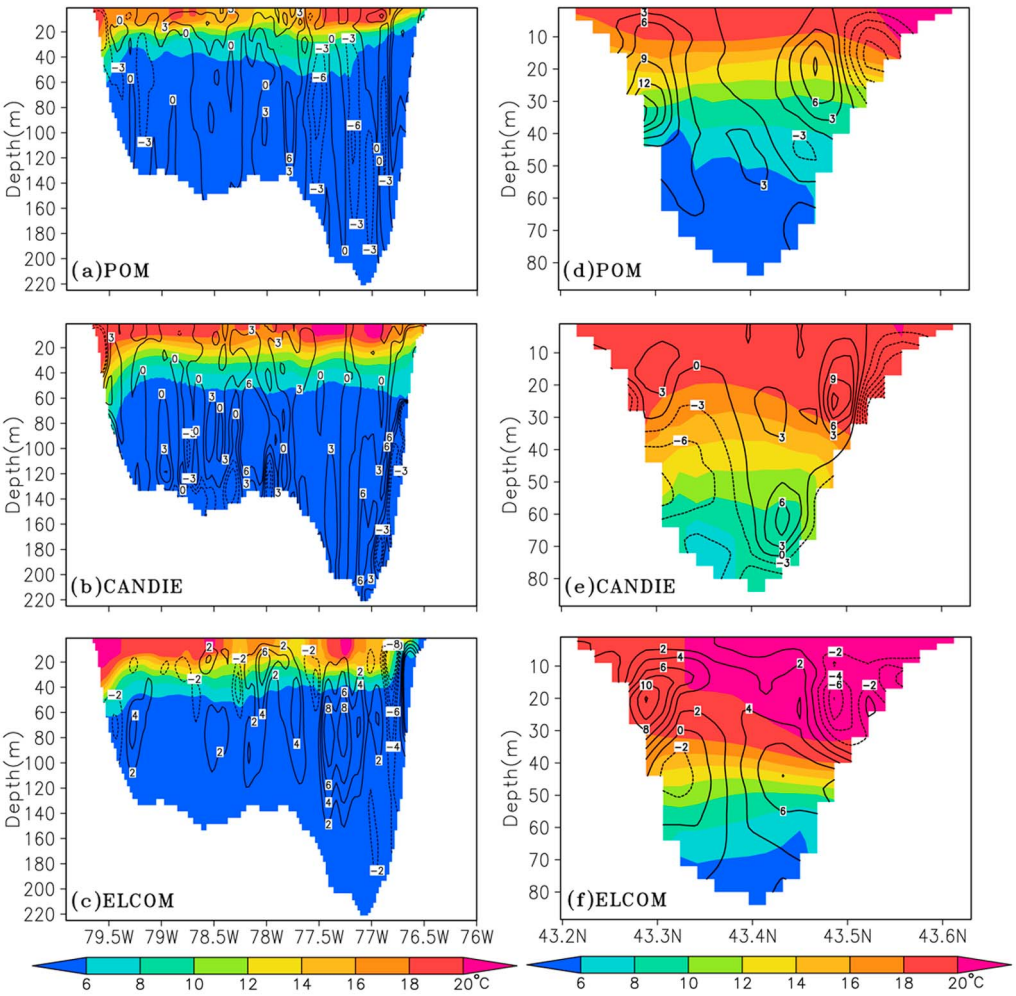

Figure 14. The modeled daily averaged water temperature (shaded, in °C) and vertical velocity (contour, in 10^{-1} cm/s and positive upward) in Lake Ontario on 1 September 2006. (left) The west-east section along 43.5°N. (right) The south-north section along 79.5°W.

the observed characteristics of temperature distribution associated with upwelling and downwelling during this episode. However, the modeled temperatures are 1°C–2°C warmer than observed values in the northeastern corner of the lake. In addition, ELCOM has 1°C–2°C warm bias in the northwestern coast of the lake; POM and ELCOM has 2°C cold bias in the southeast shore. Compared with POM and ELCOM, CANDIE obtained weaker spatial variations in surface temperature.

[29] The modeled near-surface currents are over laid on temperature distributions in Figure 13. The general patterns are similar, but differences are also quite noticeable. The solutions of POM and CANDIE are similar, both consisting westward jets with magnitude over 20 cm/s in the southeast and northwestern shores. The observed currents on this day are of similar magnitude flowing to the west in the western Lake Ontario (see Figure 8). POM and ELCOM produced a cyclonic gyre in the western corner of the lake. ELCOM obtained similar northwestward currents as POM and CANDIE along the southeastern shore; however, the magnitude of current in the midlake is much larger than that from POM and CANDIE.

[30] The lake response to meteorological forcing during this event is further assessed by examining the distributions of temperature and flow along two cross sections of the lake. For comparison with mooring observations, we chose the west-east section along the latitude of 43.5°N and south-north section along the longitude of 79.5°W, respectively. Figures 14a–14c show the simulated temperature and vertical velocity in the west-east cross section. All the three models showed downwelling in the western part of the lake, with the thermocline located at the depth of 40–45 m that is comparable to observations. The surface temperatures in the downwelling zone were close to 20°C. All the models obtained downward vertical velocities on the order of 0.1–0.2 cm/s very close to the shoreline. Upwelling occurred on the eastern shore and in the region between 76.5°W and 77°W. On the eastern shore, in the ELCOM solution the thermocline was surfaced at a distance of 4–6 km offshore and the near-surface temperatures dropped to less than 8°C. Although POM also showed rising thermocline near the surface, the simulated surface temperature in this region agrees well with observations (Figure 12a). Both POM and ELCOM showed midlake upwelling near 78°W, consistent with the AVHRR observa-

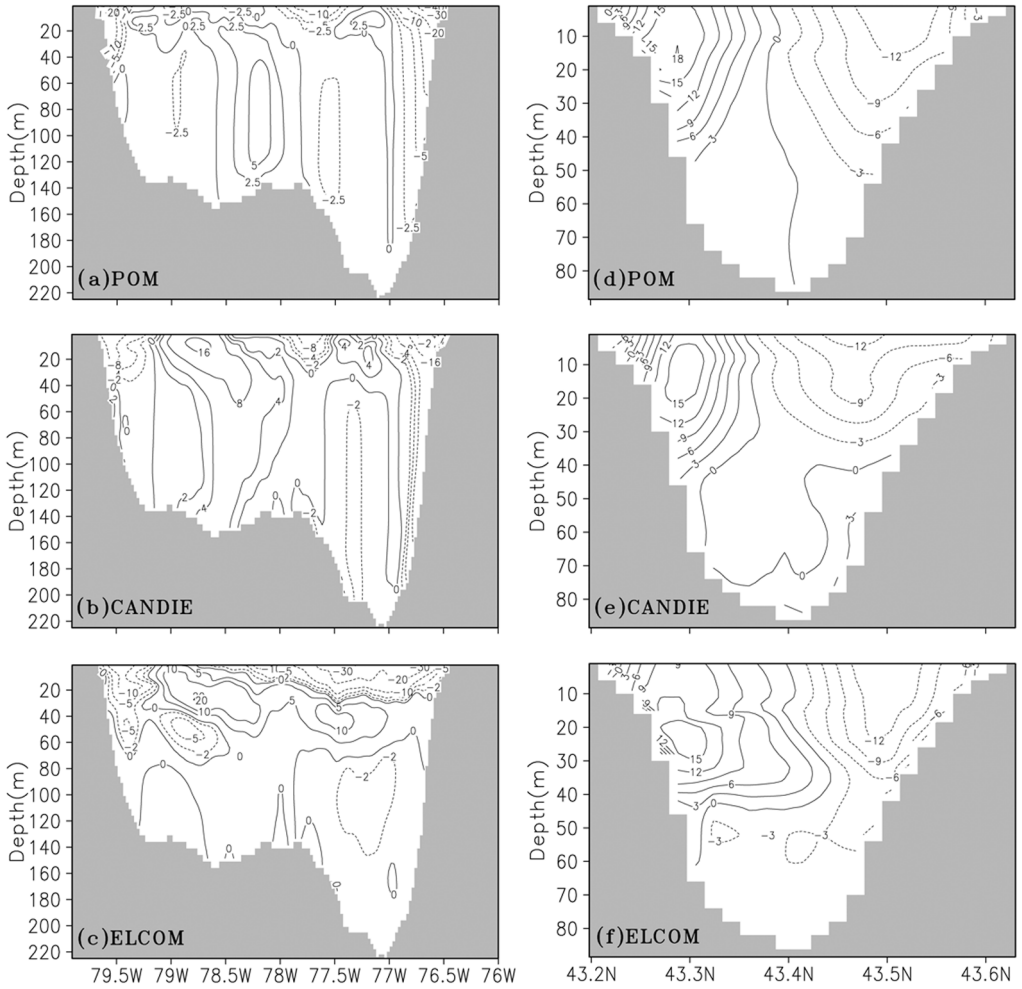

Figure 15. Same as Figure 14, except for the daily averaged *u* component of flow (positive eastward), in cm s^{-1}.

tions on this day. The coastal upwelling velocities are about 0.6 cm/s in the solution of ELCOM but are much smaller in the solutions of POM and CANDIE. Along the north-south cross section (Figures 14d–14f), the signals of upwelling and downwelling are more pronounced in the solutions of all the three models. POM and ELCOM obtained upwelling velocities over 1 cm/s in magnitude. ELCOM and CANDIE produced very strong downwelling velocities along the north shore, where the thermocline was located near 50 m depth. No significant upwelling of isotherms was simulated in the south shore. This is expected because in this region downwelling was more dominant than upwelling. Furthermore, the results of CANDIE showed more diffused thermocline, with the 10° C–12°C isotherms reaching near the bottom along the north shore. Although both ELCOM and CANDIE use the same *z* levels in the vertical, the solution of ELCOM is closer to observations than CANDIE.

[31] The vertical structure of horizontal currents along the east-west cross section is shown in Figures 15a–15c. POM and CANDIE obtained similar distributions of the *u* component velocity with wave-like structures in the midlake. Both models show strong westward currents, causing upwelling in the eastern and downwelling in western ends of the lake. ELCOM produced westward currents along the surface layer and eastward velocity at subsurface layers, indicating a two-layered structure of the flow. The *u* component velocity along the north-south cross section is shown in Figures 15d–15f. All the three models produced similar structure of the flow, with westward currents in the order of 12–13 cm s^{-1} along the north shore, in good agreement with the observations at station 1270 (see Figure 8). Along the south shore, the currents are in the eastward direction, indicating a cyclonic flow. The comparison of offshore currents along the north-south cross section shows similar characteristics among the models (figures not shown).

6. Conclusions

[32] The solutions of three lake hydrodynamic models, POM, ELCOM, and CANDIE, are compared with each other and with observations in Lake Ontario. All models have a uniform horizontal grid size of 2 km and forced by meteorological observations during mid-April to early October of 2006. The three models obtained qualitatively similar results, although they have differences in physical parameters, numerical scheme, and vertical discretization (Table 1). Comparison

with observations shows that the three models can reproduce the time evolution of lake surface temperature reasonably well. The lake surface temperatures from POM and CANDIE are closer to each other and agree better with the observations than that from ELCOM, which has a noticeable cold bias during summer at some stations and in the lake-wide average. All the models produced shallower mixed layers than observations at midlake stations but performed better near the coast. The models did not include vertical mixing due to surface waves and Langmuir circulations, and this may contribute to the underestimation of the mixed layer depths. All models had large errors in simulating the temperatures in the thermocline, associated with errors in simulating the depth of the mixed layer. Using σ or z levels, the models all showed diffused thermoclines. This indicates that differences in the simulated temperature distribution may be more related to differences in the parameterization of vertical mixing, instead of that in the vertical discretization. Numerical diffusion in these models may also be different, but such difference is not straightforward to quantify. The results from the intercomparison suggest that the vertical mixing schemes in these models have their limitations and need to be further examined and improved. All the models reproduced the characteristics of the time variability of the observed currents. The statistics of the normalized Fourier norms show that the models had substantial error in simulating subsurface currents, with POM performing slightly better.

[33] The three models all reproduced the observed spatial pattern of the summer mean near-surface temperatures, with upwelling (colder temperatures) along the north shore and downwelling (warmer temperatures) along the southeastern shore. All models simulated a distinct lake-wide cyclonic circulation occupying a large portion of the lake, and ELCOM and POM also obtained a smaller anticyclonic gyre in the western corner of the lake. The anticyclonic gyre did not exist in the solution of CANDIE. The patterns of the summer mean currents obtained by the models are in good agreement with the observed climatology. In terms of the magnitudes of the current, ELCOM obtained too strong near-surface currents in midlake and depth-averaged currents along the north shore, whereas the solutions of POM and CANDIE agreed better with observations.

[34] The models are further compared in their simulations of upwelling and downwelling processes in the lake during a strong easterly wind event. The performances of the models are qualitatively similar and agree with the expected dynamic response to the strong wind forcing. The model-simulated lake-wide distributions of temperature agree well with satellite and mooring observations. The horizontal and vertical currents are consistent with the wind-forced dynamics. The intercomparison results suggest that the lake hydrodynamic models are capable of simulating the temporal and spatial variations of temperatures and currents in large lakes. This encourages us to further test the coupling of them with the atmospheric models.

[35] **Acknowledgments.** We thank the Centre for Water Research, University of Western Australia for providing access to ELCOM model and William Schertzer for providing comments on an earlier version of the manuscript. We thank Songzhi Liu for providing CoastWatch data. We also thank Frank Bryan and two anonymous reviewers for providing constructive comments that helped improve the original manuscript. The first author acknowledges the support by National Natural Science Foundation of China (grant 40805041).

References

Anyah, R. O., and F. H. M. Semazzi (2004), Simulation of the sensitivity of Lake Victoria basin climate to lake surface temperatures, *Theor. Appl. Climatol.*, *79*, 55–69, doi: 10.1007/s00704-004-0057-4.

Baptista, A. M., E. E. Adams, and P. Gresho (1995), Benchmarks for the transport equation: The convective diffusion forum and beyond, in *Quantitative Skill Assessment for the Coastal Ocean Models*, vol. 47, edited by D. Lynch and A. Davies, pp. 241–268, AGU, Washington, D. C.

Beckers, J. M., et al. (2002), Model intercomparison in the Mediterranean: MEDMEX simulations of the seasonal cycle, *J. Mar. Syst.*, *33*, 215–251.

Beletsky, D., and D. J. Schwab (2001), Modeling circulation and thermal structure in Lake Michigan: Annual cycle and interannual variability, *J. Geophys. Res.*, *106*(C9), 19,745–19,771, doi:10.1029/2000JC000691.

Beletsky, D., W. P. O'Connor, D. J. Schwab, and D. E. Dietrich (1997), Numerical simulation of internal Kelvin waves and coastal upwelling fronts, *J. Phys. Oceanogr.*, *27*, 1197–1215.

Beletsky, D., J. H. Saylor, and D. J. Schwab (1999), Mean circulation in the Great Lakes, *J. Great Lakes Res.*, *25*, 78–93.

Beletsky, D., D. J. Schwab, and M. McCormick (2006), Modeling the 1998–2003 summer circulation and thermal structure in Lake Michigan, *J. Geophys. Res.*, *111*, C10010, doi:10.1029/2005JC003222.

Bennett, J. R. (1977), A three-dimensional model of Lake Ontario's summer circulation: I. comparison with observations, *J. Phys. Oceanogr.*, *7*, 591–601.

Blumberg, A. F., and G. L. Mellor (1987), A description of a three-dimensional coastal ocean circulation model, in *Three-Dimensional Coastal Ocean Models*, vol. 4, edited by N. Heaps, 208 pp., AGU, Washington, D. C.

Boyce, F. M., M. A. Donelan, P. F. Hamblin, C. R. Murthy, and T. J. Simos (1989), Thermal structure and circulation in the Great Lakes, *Atmos. Ocean*, *27*(4), 607–642.

Casulli, V., and R. T. Cheng (1992), Semi-implicit finite difference methods for three-dimensional shallow water flow, *Int. J. Numer. Methods Fluids*, *15*, 629–648.

Chassignet, E. P., H. Arango, D. Dietrich, T. Ezer, M. Ghil, D. B. Haidvogel, C. C. Ma, A. Mehra, A. M. Paiva, and Z. Sirkes (2000), DAMÉE-NAB: The base experiments, *Dyn. Atmos. Ocean*, *32*, 155–183.

Craig, P. D., and M. L. Banner (1994), Modeling wave-enhanced turbulence in the ocean surface layer, *J. Phys. Oceanogr.*, *24*, 2546–2559.

Davies, A., and J. Xing (1995), An intercomparison and validation of range of turbulence schemes used in three-dimensional tidal models, in *Quantitative Skill Assessment for the Coastal Ocean Models*, vol. 47, D. Lynch and A. Davies, pp. 71–95, AGU, Washington, D. C.

Dietrich, D. E. (1997), Application of a modified Arakawa a grid ocean model having reduced numerical dispersion to the Gulf of Mexico circulation, *Dyn. Atmos. Oceans*, *27*, 101–217.

Ezer, T. (2000), On the seasonal mixed layer simulated by a basin-scale ocean model and the Mellor-Yamada turbulence scheme, *J. Geophys. Res.*, *105*(C7), 16,843–16,855, doi:10.1029/2000JC900088.

Ezer, T. (2005), Entrainment, diapycnal mixing and transport in three-dimensional bottom gravity current simulations using the Mellor-Yamada turbulence scheme, *Ocean Modell.*, *9*, 151–168.

Ezer, T., and G. L. Mellor (2004), A generalized coordinate ocean model and a comparison of the bottom boundary layer dynamics in terrain-following and in z level grids, *Ocean Modell.*, *6*(3–4), 379–403.

Fischer, H. B., E. G. List, R. C. Y. Koh, J. Imberger, and N. H. Brooks (1979), *Mixing in Inland and Coastal Waters*, 28 pp., Academic, New York.

Hanrahan, J. L., S. V. Kravtsov, and P. J. Roebber (2010), Connecting past and present climate variability to the water levels of Lakes Michigan and Huron, *Geophys. Res. Lett.*, *37*, L01701, doi:10.1029/2009GL041707.

Hodges, B. R., and C. Dallimore (2006), *Estuary, Lake and Coastal Ocean Model: ELCOM, Users Guide*, 62 pp., Cent. for Water Res., Univ. of Western Australia Tech. Publ., Perth, Australia.

Hodges, B. R., J. Imberger, A. Saggio, and K. B. Winters (2000), Modelling basin scale internal waves in a stratified lake, *Limnol. Oceanogr.*, *45*(7), 1603–1620.

Huang, A., Y. R. Rao, and Y. Lu (2010), Evaluation of a 3-D hydrodynamic model and atmospheric forecast forcing using observations in Lake Ontario, *J. Geophys. Res.*, *115*, C02004, doi:10.1029/2009JC005601.

Jerlov, N. G. (1976), *Marine Optics*, 231 pp., Elsevier, New York.

King, J. R., B. J. Shuter, and A. P. Zimmerman (1997), The response of the thermal stratification of South Bay (Lake Huron) to climatic variability, *Can. J. Fish. Aquat. Sci.*, *54*, 1873–1882.

Kuan, C., K. W. Bedford, and D. J. Schwab (1994), A preliminary credibility analysis of the Lake Erie portion of the Great Lakes Forecasting System for springtime heating conditions, in *Quantitative Skill Assessment for Coastal*

Ocean Models, *Coastal Estuarine Stud.*, vol. 47, edited by D. R. Lynch and A. M. Davies, pp. 397–423, AGU, Washington, D. C.

Lam, D. C. L., and W. M. Schertzer (1999), *Potential Climate Change Effects on Great Lakes Hydrodynamics and Water Quality*, 232 pp., ASCE, Reston, Va.

Large, W. G., and S. Pond (1981), Open ocean momentum flux measurements in moderate to strong winds, *J. Phys. Oceanogr.*, *11*, 324–336.

Large, W. G., J. C. McWilliams, and S. C. Doney (1994), Oceanic vertical mixing: A review and a model with nonlocal boundary layer parameterization, *Rev. Geophys.*, *32*, 363–403.

Laval, B., J. Imberger, B. R. Hodges, and R. Stocker (2003), Modelling circulation in lakes: Spatial and temporal variations, *Limnol. Oceanogr.*, *48*, 983–994.

Legg, S., R. Hallberg, and J. Girton (2006), Comparison of entrainment in overflows simulated by z-coordinate, isopycnal and nonhydrostatic models, *Ocean Modell.*, *11*, 69–97.

Leon, L., J. Imberger, R. E. H. Smith, R. E. Hecky, D. C. L. Lam, and W. M. Schertzer (2005), Modelling as a tool for nutrient management in Lake Erie: A hydrodynamics study, *J. Great Lakes Res.*, *31*(2), 309–318.

Long, Z., W. Perrie, J. Gyakum, D. Caya, and R. Laprise (2007), Northern lake impacts on local seasonal climate, *J. Hydrometeorol.*, *8*, 881–896.

Lu, Y., D. G. Wright, and D. Brickman (2001), Internal tide generation over topography: Experiments with a free-surface *z* level ocean model, *J. Atmos. Oceanic Technol.*, *18*, 1076–1091.

McCormick, M. J., and G. A. Meadows (1988), An intercomparison of four mixed layer models in a shallow inland sea, *J. Geophys. Res.*, *93*(69), 6774–6788, doi:10.1029/JC093iC06p06774.

Mellor, G. L. (2004), *Users' Guide for a Three-Dimensional, Primitive Equation, Numerical Ocean Model (June 2004 version)*, 42 pp., Princeton Univ. Press, Princeton.

Mellor, G. L. (2008), The depth-dependent current and wave interaction equations: A revision, *J. Phys. Oceanogr.*, *38*, 2587–2596.

Mellor, G. L., and A. F. Blumberg (1985), Modelling vertical and horizontal diffusivities with the σ coordinate system, *Mon. Weather Rev.*, *113*, 1380–1383.

Mellor, G. L., and A. Blumberg (2004), Wave breaking and ocean surface thermal response, *J. Phys. Oceanogr*, *34*, 693–698.

Mellor, G. L., and T. Yamada (1982), Development of a turbulence closure model for geophysical fluid problems, *Rev. Geophys.*, *20*, 851–875.

Mellor, G. L., S. Hakkinen, T. Ezer, and R. Patchen (2002), A generalization of a σ coordinate ocean model and an intercomparison of model vertical grids, in *Ocean Forecasting: Conceptual Basis and Applications*, edited by N. Pinardi and J. D. Woods, 55–72, Springer, Berlin.

Obolkinm, V. A., and V. L. Potemkin (2006), The impact of large lakes on climate in the past: A possible scenario for Lake Baikal, *Hydrobiologia*, *568*(S), 249–252.

Pellerin, P., H. Ritchie, F. J. Saucier, F. Roy, S. Desjardins, M. Valin, and V. Lee (2004), Impact of a two-way coupling between an atmospheric and ocean-Ice model over the Gulf of St. Lawrence, *Mon. Weather Rev.*, *132*, 1379–1398.

Rao, Y. R., and C. R. Murthy (2001), Nearshore currents and turbulent exchange characteristics during upwelling and downwelling events in Lake Ontario, *J. Geophys. Res.*, *106*(C2), 2667–2678, doi:10.1029/2000JC900149.

Rao, Y. R., C.H. Marvin, and J. Zhao (2009), Application of a numerical model for circulation, temperature and pollutant distribution in Hamilton Harbour, *J. Great Lakes Res.*, doi:10.1016/j.jglr.2008.09.004

Saylor, J. H., J. R. Bennet, F. M. Boyce, C. R. Murthy, R. L. Picket, and T. J. Simons (1981), Water movements, in *IFYGL-International Field Year on the Great Lakes*, edited by E. J. Aubert and T. L. Richards, pp. 7–32, Great Lakes Environ. Lab., Ann Arbor, Mich.

Schwab, D. J., and K.W. Bedford (1994), Initial implementation of the Great Lakes forecasting system: A real-time system for predicting lake circulation and thermal structure, *Water Pollut. Res. J. Can.*, *29*, 203–220.

Sheng, J., and Y. R. Rao (2006), Circulation and thermal structure in Lake Huron and Georgian Bay: Application of a nested grid hydrodynamic model, *Cont. Shelf Res.*, *26*, 1496–1518.

Sheng, J., G. Wright, R. J. Greatbatch, and D. Dietrich (1998), CANDIE: A new version of the DieCAST ocean circulation model, *J. Atmos. Ocean. Technol.*, *15*, 1414–1432.

Simons, T. J. (1980), Circulation models of lakes and inland seas, *Can. Bull. Fish. Aquat. Sci.*, *203*, 146.

Smagorinsky, J. (1963), General circulation experiments with the primitive equation: I. The basic experiment, *Mon. Weather Rev.*, *12*, 99–165.

Song, Y., F. H. M. Semazzi, L. Xie, and L. J. Ogallo (2004), A coupled regional climate model for the Lake Victoria Basin of East Africa, *Int. J. Climatol.*, *24*, 57–75.

Thuburn, J. (1996), Multidimensional flux-limited advection schemes, *J. Comput. Phys.*, *123*, 74–83.

A. Huang, School of Atmospheric Sciences, Nanjing University, 22, Hankou Road, Nanjing, China 210093.

Y. Lu, Department of Fisheries and Oceans, Bedford Institute of Oceanography, 1 Challenger Dr., Dartmouth, NS B2Y 4A2, Canada.

Y. R. Rao and J. Zhao, National Water Research Institute, Water Science and Technology Directorate, Environment Canada, 867 Lakeshore Road, Burlington, ON L7R 4A6, Canada. (ram.yerubandi@ec.gc.ca)